

K. O'KEEFFE<sup>1</sup>  
P. JÖCHL<sup>1</sup>  
H. DREXEL<sup>2</sup>  
V. GRILL<sup>2</sup>  
F. KRAUSZ<sup>1</sup>  
M. LEZIUS<sup>1,2,✉</sup>

# Carrier-envelope phase measurement using a non phase stable laser

<sup>1</sup> Photonics Institute, Vienna Technical University, Gusshausstr. 27/387, 1040 Vienna, Austria  
<sup>2</sup> Ion Physics Institute, Innsbruck University, Technikerstr. 25, 6020 Innsbruck, Austria

Received: 7 August 2003/Revised version: 15 January 2004  
Published online: 5 March 2004 • © Springer-Verlag 2004

**ABSTRACT** We demonstrate that the phase between the carrier and the pulse envelope of a few-cycle laser pulse can be retrieved from non phase stable laser systems, provided that such laser pulses are about 5 fs long and the repetition rate is in the order of 1 kHz. Our approach is based on online determination of the phase using  $f - 2f$  interferometry. By a comparison of the self referencing interferometric signal with the photoelectron current emitted into a 7 degree solid angle parallel to the laser polarization, we obtain the absolute value of the carrier envelope phase. This is provided that a Coulomb correction for electron energies below 10 eV can be correctly taken into account.

PACS 42.50.Hz; 42.65.Re; 32.80.Rm

## 1 Introduction

When the duration of laser pulses reaches the current frontier of approximately two optical cycles, it makes a difference to many processes at which phase the carrier frequency of the electromagnetic field wave is situated with respect to the pulse envelope. The present convention is, if the carrier wave peaks at the peak of the envelope, we call this a cosine wave with the carrier envelope phase (CE-phase)  $\varphi = 0$ . If the carrier peak is shifted by  $\pi/2$  with respect to the peak of the envelope, we call this a sine wave. The shape of sine and cosine waves differ strongly in the few cycle regime and therefore significantly influences the way in which matter responds to the field. The measurement and/or the control of the CE-phase is therefore a fundamental requirement for coherent control in the few-cycle regime, and it opens the door for so-called single cycle ionization. In this respect, the CE-phase is situated at the very heart of modern attosecond technology and metrology [1–4], where promising schemes are based on the creation of attosecond electron wave packets (attosecond ionization bursts) that can be precisely controlled in time and space by the field strength and the CE-phase [4].

It has been demonstrated by Reichert et al. [5] and by Jones et al. [6] that the CE-phase can be stabilized using

a Mach-Zender interferometer with subsequent feedback of a heterodyne signal into the oscillator pump. A similar system with an extended oscillator cavity length has been built in Vienna. In the meantime such laser systems have become commercially available, and stabilization times are reaching several minutes [7], for a more recent review see [8]. The phase-slip of such oscillators is only locked to a fraction of the oscillator frequency, meaning that from shot to shot the phase varies strongly, therefore proper pulse selection techniques have to be applied. Recent works have demonstrated that the CE-phase can now be stabilized within an accuracy of about 0.5 rad [9]. The stability of the CE-phase can be measured using the  $f - 2f$  interference technique, as pioneered by Mehendale [10] and Kakehata [11]. With respect to atomic physics it was up to now impossible to increase the typical pulse energy (several nJ) of phase stabilized oscillator systems by increasing the cavity length into a range where strong field experiments become attractive. It is nevertheless possible to amplify laser pulses from phase stable oscillators if the additional phase drift is stabilized using a second feedback loop. This was demonstrated recently by A. Baltuska et al. [4] and resulted in 5 fs pulses with a power approaching the mJ (TW) range. The technique proved to be a valuable tool for several current research topics on CE-phase effects. Such typical CE-phase dependent rescattering processes are high order harmonic generation (HHG), above threshold ionisation (ATI), and non-sequential double ionisation (NSDI). In HHG it was for example demonstrated that in contrast to cosine pulses only sine pulses from a CE-phase stabilized system produce a single attosecond XUV laser pulse (compared to a double pulse train in the cosine case) [4]. This is of relevance for many experimental schemes based on an attosecond excitation (pump) followed by an ultrashort probe pulse [2]. Regarding the other hand ATI, it has been predicted by various authors [12–15] that the spatial ejection of ATI-electrons should depend on the CE-phase. This effect was demonstrated in a stereo-ATI experiment using correlation techniques for a non phase stable laser [16]. With only very few modifications the same stereo-ATI experiment has just demonstrated that the absolute CE-phase can be measured with an unprecedented precision [17, 18]. Moreover, performing stereo-ATI under the use of CE-phase stabilized few-cycle pulses has shed light onto subtle differences between the trajectories of so-called direct and indirect (or rescattered) ATI electrons.

✉ Fax: +43-1/58801-38799, E-mail: matthias.lezius@tuwien.ac.at

The ATI plateau region and the high energy cut-off of typical ATI spectra consists of electrons which were produced at the peak intensity of the electric field and then rescattered on the parent ion core upon return after one optical half-cycle [19]. As a consequence, these high energy electrons are in phase with the CE-phase so that the cut-off moves to higher electron energies for the case of a cosine pulse while it moves to lower energies for a sine pulse. From recent results obtained in [17] it appears that for energies below  $\approx 10$  eV the Coulomb potential produced by the remaining ion core influences the ejected electron current. Therefore it is necessary to include a Coulomb correction in order to determine the exact value of the CE-phase. It is not yet quite clear how this effect depends on various parameters such as target gas, intensity and pulse duration. Our present solution to such an uncertainty is pragmatic: we use the same target gas and a similar intensity as has been used in [17], which we can then use for calibration. The exact determination of the CE-phase, as it was demonstrated in [17], opens many opportunities for exact timing and control in the attosecond time domain, and of course for coherent control in the few cycle regime. It has been observed in [4] that for the case of few-cycle sine pulses subsequent rescattering can be significantly reduced (perhaps even totally suppressed), so that true single cycle ionization within a few 100 as becomes possible. Without doubt the measurement of the CE-phase is of enormous importance to the ultrafast laser community and has also in many senses paved the way for the technique demonstrated here. Nevertheless, in contrast to [17, 18] the present work presents a greatly simplified approach for CE-phase measurements. We show here that in many laser systems the phase stabilization of the laser can be omitted, if one is capable of measuring and interpreting the relative CE-phase online by using an  $f - 2f$  interferometer setup similar to that used by Kakehata et al. [11]. This can be done for pulse repetition rates of at least up to 1 kHz, possibly even up to 5 kHz, which represent the majority of amplified few-cycle systems. With our technique CE-phase dependent physics becomes available to many laboratories having few-cycle pulsed laser systems at hand but which have not implemented a laser phase stabilization scheme yet.

## 2 Experimental

We have used a home-built laser system that has been constructed and described in detail previously [20]. A 20-fs seed from a (FemtoLaser) oscillator is stretched using 20 mm glass and injected at a 1 kHz rate into a 10 pass amplifier system. The resulting pulse (1.3 mJ) is recompressed to about 25 fs and focussed into a 1 m long hollow fibre of 180  $\mu\text{m}$  diameter, filled with 1.5 bar neon gas. Due to self-phase modulation [21] this produces a spectrally broadened laser pulse ( $\approx 500 \mu\text{J}$ ) that can be recompressed down to approximately 10 fs using chirped multilayer mirrors. A split of 18% is then taken and its polarization is cleaned using three consecutive pellicles at the brewster angle. About 30  $\mu\text{J}$ /pulse at 10 fs are then available for the experiment, illustrated in Fig. 1. These pulses are injected ( $f = -500$  mm) into a second hollow fibre (C) of 166  $\mu\text{m}$  diameter and 70 mm length. This hollow fibre is filled with 2.5 bar of krypton gas. It can be seen in Fig. 2 that after the fibre the laser pulse is spec-

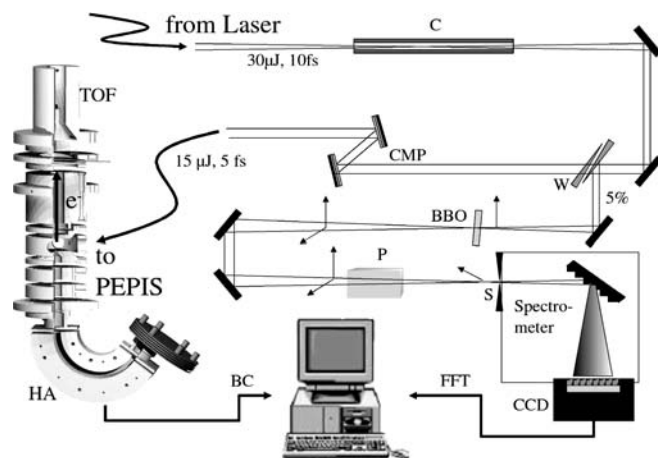


**FIGURE 1** Sketch of the experimental setup used for determining the carrier envelope phase. The laser pulses are spectrally broadened up to one octave (see Fig. 3). Then the beam is split into two parts, a weak part that is used for  $f - 2f$  interferometry and an intense part that is compressed to 5 fs and used to produce ATI electrons from a low pressure Xenon gas target in a photoelectron spectrometer (PEPIS, left side). Electron current and CE-phase from the  $f - 2f$  interferometer are stored and compared online on a computer (see text)

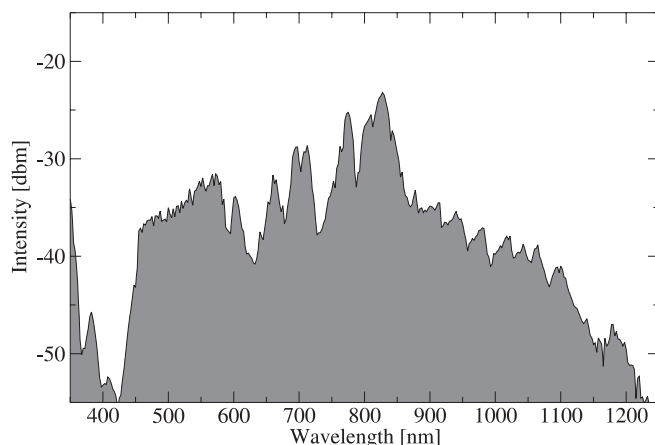


**FIGURE 2** Typical spectrum of the laser pulse obtained after a 7 cm long 166  $\mu\text{m}$  hollow fibre filled with 2.5 bar Krypton. The spectral bandwidth reaches up to two octaves and can be used for  $f - 2f$  interferometry and to compress pulses down to approximately 5 fs

trally broadened from 400 to 1200 nm, which is necessary for efficient  $f - 2f$  interferometry and for successful compression into the few-cycle regime. For pulse compression a pair of fused silica thin wedges (W) were used for fine tuning of the group velocity dispersion in front of a broadband multilayer mirror compressor (CMP). After compression the pulse form and duration can be monitored using a broad bandwidth, dispersion-free interferometric autocorrelation, capable of handling more than one octave bandwidth. This autocorrelator is described in [22]. The autocorrelator has been positioned at the same distance of optical path from the compressor as the electron spectrometer (PEPIS) described below. A typical autocorrelation is shown in Fig. 3. However it should be stressed that such autocorrelations at best only yield a rough estimate of the pulse duration. For a more accurate determination of the pulse duration it is necessary to use a more sophisticated pulse diagnostic such as SPIDER [23]. In this experiment the pulse duration was first roughly opti-

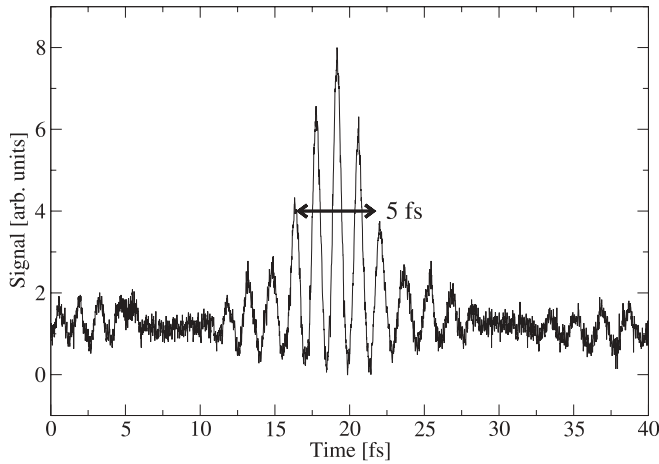


**FIGURE 3** Typical autocorrelation for the laser pulses used in the present experiment

mised by using autocorrelation and was then fine tuned by observing the electron signal and adjusting the wedge insertion accordingly.

5% reflection ( $\approx 600$  nJ) from the first surface of the pair of wedges is used for our  $f - 2f$  interferometer. This part of the beam is focussed by a  $f = -200$  mm spherical mirror into a  $100 \mu\text{m}$  BBO type II crystal. The resulting copropagating  $f$  and  $2f$  beams are sent through a Glan-Thompson polarizer (P) and then refocused ( $f = 250$  mm) into the  $5\text{--}500 \mu\text{m}$  adjustable slit (S, usually set close to  $5 \mu\text{m}$ ) of a spectrometer (MS125 ORIEL). Similar  $f - 2f$  interferometry has been described in [11]. The resolution of the spectrometer is about  $1 \text{ nm}$ , using a  $6001/\text{mm}$  grating ( $400 \text{ nm}$  Blaze) and a  $1024$  pixel ( $10 \mu\text{m}^2$ ) laser clocked linescan CCD camera (Basler L102). The CCD can be read with line rates up to  $35 \text{ kHz}$ . In the present case the number of pixels used for evaluation was reduced to  $256$ , e.g. every second pixel was used for a region covering half the sensor size (software adjustable). The camera is read within  $65 \mu\text{s}$  by a digital frame-grabber (National Instruments, PCI-1422). Typical spectra like those shown in Fig. 4 are fast-fourier-transformed online in less than  $500 \mu\text{s}$  using LabView 6i FFT routines. The resulting power spectrum (see insert in Fig. 4) shows a distinguished peak, at which the CE-phase  $\Phi$  can be evaluated. This phase should not be confused with the absolute CE-phase since it is only the pulse to pulse change of the phase and not its absolute value. Nevertheless, in the absence of excessive extracavity drifts in the offset constant  $\Phi_0$  it is correlated between  $0$  and  $2\pi$  by  $\varphi = \Phi + \Phi_0$  [24]. Regarding the data acquisition software, in the present set-up we have coded all data acquisition and evaluation in LabView 6i, with some additionally embedded dynamic link libraries for a high-precision boxcar card.

To detect the spatial dependence of electrons produced via ATI we use a small photo-electron photo-ion spectrometer (PEPIS). This spectrometer consists of two arms: The electron spectrometer itself is based on a hemispherical analyzer (HA, COMSTOCK AC-900, center radius  $18.3 \text{ mm}$ ). The second arm of the PEPIS consists of a short time-of-flight spectrometer (TOF) with a drift tube of  $25 \text{ mm}$  in length and equipped with a home-made bipolar detector. This arm is normally used for ion and charge state detection, but it was

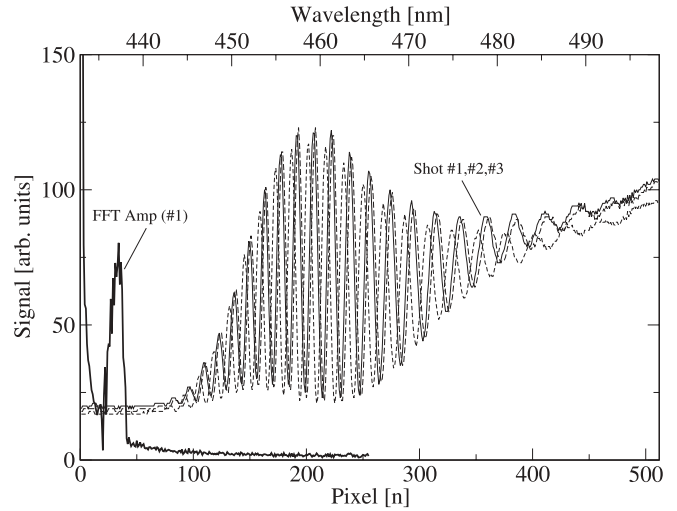


**FIGURE 4** Typical  $f - 2f$  interferometric spectrum used for determination of the relative CE-phase in the present experiment. For each laser shot the interference pattern varies, using a non-stable laser system. These spectra were evaluated using fast-fourier transformation (FFT), and the relative phase  $\Phi$  was evaluated at the center of the peak in the power FFT spectrum (shown left)

used here for the detection of electrons. The left side of Fig. 1 shows a schematic view of the PEPIS ion optics arrangement. The laser beam is focussed close to the center of the spectrometer with a  $70 \text{ mm}$  spherical mirror (back-reflection mode,  $F \approx 20$ ). The position of the focus was slightly tuned away with respect to the  $500 \mu\text{m}$  electron exit aperture. This is necessary in order to reduce the intensity down to approximately  $2 \times 10^{14} \text{ W/cm}^2$  and to avoid effects of the Gouy-phase [25]. As a typical target gas we have chosen  $2 \times 10^{-6}$  mbar of xenon introduced via a  $200 \mu\text{m}$  precision controlled capillary inlet system. The residual gas pressure of the system was in the order of  $5 \times 10^{-10}$  mbar. In ion-TOF detection mode we were able to detect a strong  $\text{Xe}^+$  signal and a weak  $\text{Xe}^{2+}$  signal (10%), which corresponds to a focal intensity of about  $2 \times 10^{14} \text{ W/cm}^2$  [26]. In electron detection mode no extraction voltages have to be applied to the liberated electrons, otherwise spatial effects which are a fingerprint for the CE-phase would be corrupted. The electron signal is measured using  $+1.8 \text{ kV}$  bias voltage on a chevron type dual-MCP detector with capacitive output coupling. Electron pulses are first pre-amplified ( $2 \text{ GHz}$  bandwidth) and then measured for each laser shot using a fast boxcar amplifier (BC, Becker&Hickl,  $250 \text{ ps}$ ). Typical detector signals are in the order of  $100 \text{ mV}$ , with a background noise of less than 10%.

### 3 Results and discussion

By tuning of the pair of wedges we have first maximized the average intensity of the electron signal which also resulted in the shortest detectable pulse in the interferometric autocorrelation. Then, during the measurement the instantaneous  $f - 2f$  relative phase value  $\Phi$  and the corresponding electron signals were stored online for each laser shot. To average out the shot-to-shot signal variation of the electron signal (in the order of 100%) it is necessary to integrate over approximately one million laser shots (20 minutes). The acquired data is immediately evaluated with a separate program.

In this program we correlate the electron signal to  $\Phi$  in a histogram of 360 bins (for  $\Phi = 0 \dots 360^\circ$ ). For each degree of  $\Phi$  all electron signals which have been measured in this phase interval are summed (resulting in an average of 2800 measurements for each of the 360 bins). During data processing we have also related the electron signal of each previous and each subsequent laser shot with the actual  $\Phi$ , thereby producing an uncorrelated histogram which makes it possible to check for a possible uncontrolled slip in the phase attribution caused by the speed maximized data-read technique. As we cannot use processor interrupt techniques here, we have to avoid that the computer reads the camera and relates it for example to an electron signal caused by the previous laser shot, an error that would not be seen by a simple control of the cycle frequency. It can be observed in Fig. 5 that the correlated and the uncorrelated histograms differ strongly. This ensures us that the  $f - 2f$  phase is correctly attributed to the electron signal. The uncorrelated histogram is additionally helpful to avoid false correlations from noisy or weakly contrasted  $f - 2f$  spectra. However, in general we are able to obtain an excellent fringe-contrast (90%) in our spectrometer, so that we obtain a comparably accurate  $f - 2f$  phase value. Note that our fringe contrast is much better than in [11], possibly because we were able to create a much broader spectrum in our hollow fibre. In addition, fringes can become much less prominent if more than one laser shot is integrated on the CCD-sensor before readout. If the fringe contrast is insufficient or if the spectrum varies strongly from one laser shot to the other, the  $f - 2f$  interferometer can not produce reliable values for  $\Phi$ . In such cases the correlated and the uncorrelated histogram look very similar.

By division of the correlated and the uncorrelated histogram we obtain the normalized and statistically corrected change of the average electron signal with the CE-phase, which turns out to be close to 10% peak-to-peak (see Fig. 6).

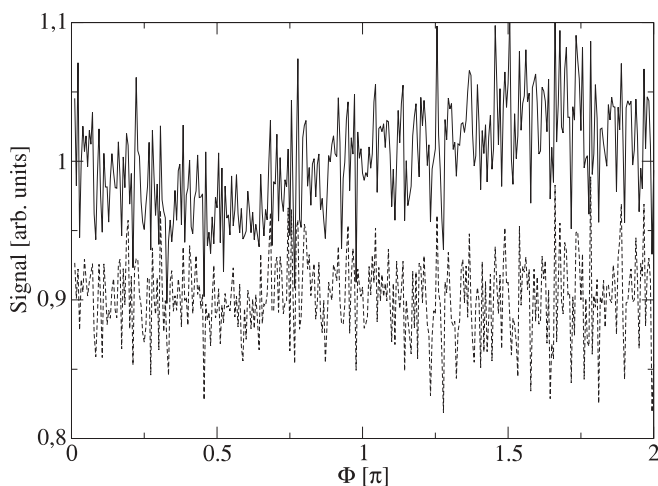


**FIGURE 5** Correlated (*full*) and uncorrelated (*dashed*) ATI electron current emitted into the 7 degree solid angle open around the laser polarization axis. In the correlated case the laser phase was determined from  $f - 2f$  interferometry of the ionizing laser pulse, while in the uncorrelated case the phase was derived from the pulse before the ionizing laser pulse. Between consecutive laser pulses the phase varies statistically. Only in the correlated case a clear CE-phase dependence is detected. The uncorrelated case has been offset by  $-0.1$  for the purpose of clarity

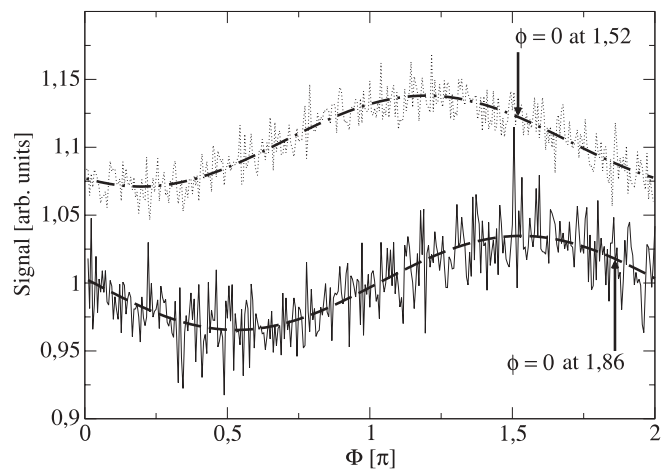


**FIGURE 6** Ratio between the uncorrelated and the correlated case for the data in Fig. 5 and an additional data set that was taken with a slightly different laser adjustment (*dotted*, offset by  $+0.1$ ). Clearly visible is a cosine-like dependence, the data can be fit by the function  $y = A0 + A1 * \cos((x - A2)\pi)$ . If a Coulomb correction is taken into account [17], the correct position for the origin of the CE-phase is at  $A2 + 0.33$ , as indicated by *arrows* in the figure

Such measurements have been reproduced many times and we can be certain that the results are statistically significant and that they are not caused by any drift of the experiment. For example, if the wedge  $W$  is slightly detuned, the origin of the CE-phase is shifted, as visible in the second data set presented in Fig. 6. It should also be pointed out that this is a variation in the signal that has been obtained via integration over a range of electron energies between  $0 \dots 10$  eV (higher electron energies are about 1000 times less probable). For the total electron yield emitted to one side our result is in excellent agreement with the results obtained from stereo-ATI [17]. As a final test of the CE-phase effect we have slightly increased the pulse duration by insertion of 0.7 mm of fused silica glass. For such a case, positive dispersion stretches the 5 fs pulse by a factor of  $\approx 1.6$  according to [27] so that CE-phase effects can be expected to vanish. This was indeed observable in similar flat histograms for both the correlated and the uncorrelated case (shown in Fig. 7).

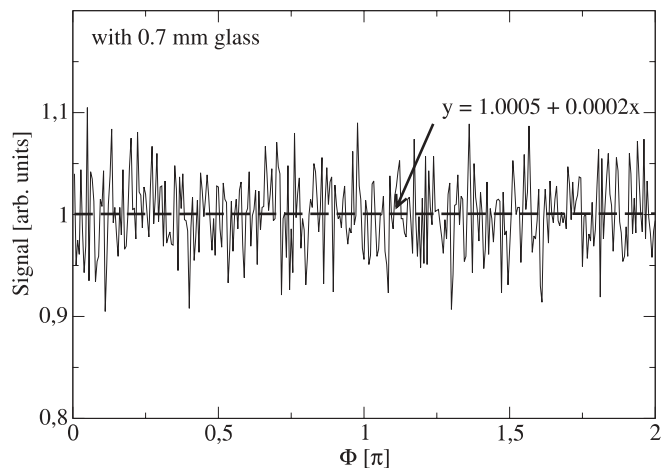


**FIGURE 7** Same measurement as shown in Fig. 5 but with 0.7 mm glass inserted into the laser beam. The additional dispersion stretches the pulse by a factor 1.6, which cancels any effects caused by the CE-phase

In contrast to stereo-ATI metrology the current system is significantly simplified because it measures only electrons scattered into one direction. Moreover, we have integrated over the total electron yield rather than determining the cut-off in the ATI energy spectra. Thus we are able to use a very compact device where the distance between the focus and the electron detector is only 25 mm. During operation the PEPIS was pumped by a small 70 l/s turbopump, so that one can imagine that even a sealed gas cell containing a standard electron multiplier could achieve a comparable performance. Because the electron current was integrated over the energy spectrum, time resolution can be reduced to the nanosecond regime, which releases restrictions in signal wiring and high performance electronics. A simple Boxcar or Lock-In technique appears sufficient to obtain similar results. Nevertheless, with our approach we are able to obtain the absolute value of the CE-phase with comparably high precision, provided that we can integrate over enough ( $10^6$ ) laser shots. If we take into account that the maximum current of low energy electrons is shifted by approximately  $\pi/3$  with respect to the optical phase  $\varphi = 0$  (derived from Fig. 3b in [17]), the position for  $\varphi = 0$  for the lower curve in Fig. 6 would be at  $\Phi = 1.86$ , as indicated. It should be noted that a more accurate value for the Coulomb correction is presently not available, this will be subject to further research by our group. Based on the technique presented here it appears possible to create an experimental setup for a single shot CE-phase measurement. For this one would calibrate the  $f - 2f$  detector with respect to the absolute CE-phase, using the present electron detection system or, alternatively, a Stereo-ATI. During experiments, calibration of the  $f - 2f$  detector would have to be remade every hour or so in order to correct for drifts in  $\Phi_0$ [24]. In this way the absolute phase would be calibrated using an average over many laser shots like in Fig. 6, while the single shot phase value is obtained online with high accuracy from the low-noise spectrometric data shown in Fig. 4.

In conclusion we have demonstrated determination of the carrier envelope phase using a fast  $f - 2f$  interferometer, a low pressure gas cell, and an electron detector for analyzing ATI electrons ejected within a restricted solid angle pointing parallel to the laser polarization axis. Phase-stabilization of the laser system becomes obsolete, which enormously relieves the constraints and the operating complexity, and which opens the door to long-term measurements. In addition, in the present work ultra-broad bandwidth generation reaching two octaves was achieved in a cascaded hollow fibre capillary setup (using an intermediate compression scheme), which could be recompressed down to pulse durations in the 5 fs range using a couple of reflections on commercially available broad bandwidth chirped multilayer mirrors. The present approach can be extended to high peak power experiments based on chained amplifier laser systems. The interferometer appeared remarkably robust against pointing instabilities as long as the broadening in the hollow fibre was not affected (in such cases a pointing stabilizer system should be used). We suggest that online  $f - 2f$  interference and CE-phase detection from ATI electrons is a powerful alternative to CE-phase stabilization.

This is especially important for cases when data acquisition needs long-term averaging over many laser shots, a typical situation when phased-locked loop stabilized lasers can easily fail to reach quality of service. Moreover, our technique can be adapted and implemented without any further modification into presently existing laser chains. Regarding laser repetition rates, using the latest high-speed 64 bit processors, we are certain that 5 kHz lasers can be serviced by the FFT routine.

**ACKNOWLEDGEMENTS** The authors are indebted to the assistance by many colleges at the Photonics Institute and the Institute for Ion Physics. Moreover, we would like to thank G.G. Paulus for enlightening discussions. This project was supported by the Austrian Funds for the Advancement of Science, project P14447 and SFB1616.

## REFERENCES

- 1 P.M. Paul, E.S. Toma, P. Breger, G. Mullot, F. Auge, P. Balcou, H.G. Müller, P. Agostini: *Science* **292**, 1689 (2001)
- 2 M. Drescher, M. Hentschel, R. Kienberger, M. Uiberacker, V. Yakovlev, A. Scrinzi, T. Westerwalbesloh, U. Kleineberg, U. Heinzmann, F. Krausz: *Nature* **419**, 803 (2002)
- 3 H. Niikura, F. Legare, R. Hasbani, M.Y. Ivanov, D.M. Villeneuve, P.B. Corkum: *Nature* **421**, 826 (2003)
- 4 A. Baltuska, T. Udem, M. Uiberacker, M. Hentschel, E. Goulielmakis, C. Gohle, R. Holzwarth, V.S. Yakovlev, A. Scrinzi, T.W. Hänsch, F. Krausz: *Nature* **421**, 611 (2003)
- 5 J. Reichert, R. Holzwarth, T. Udem, T.W. Hänsch: *Opt. Commun.* **172**, 59 (1999)
- 6 D.J. Jones, S.A. Diddams, J.K. Ranka, A. Stentz, R.S. Windeler, J.L. Hall, S.T. Cundiff: *Science* **288**, 635 (2000)
- 7 T.M. Fortier, D.J. Jones, Jun Ye, S.T. Cundiff, R.S. Windeler: *Opt. Lett.* **27**, 1436 (2002)
- 8 S.T. Cundiff: *J. Phys. D: Appl. Phys.* **35**, R43 (2002)
- 9 T.M. Fortier, Jun Ye, S.T. Cundiff, R.S. Windeler: *Opt. Lett.* **27**, 445 (2002)
- 10 M. Mehendale, S.A. Mitchell, J.P. Likforman, D.M. Villeneuve, P.B. Corkum: *Opt. Lett.* **25**, 1672 (2000)
- 11 M. Kakehata, H. Takada, Y. Kobayashi, K. Torizuka, Y. Fujihira, T. Homma, H. Takahashi: *Opt. Lett.* **26**, 1436 (2001)
- 12 E. Cormier, P. Lambropoulos: *Eur. Phys. J. D* **2**, 15 (1998)
- 13 P. Dietrich, F. Krausz, P.B. Corkum: *Opt. Lett.* **25**, 16 (2000)
- 14 I.P. Christov: *Appl. Phys. B: Lasers Opt.* **B70**, 459 (2000)
- 15 R.M. Potvliege, N.J. Kylstra, C.J. Joachain: *J. Phys. B: At. Mol. Opt. Phys.* **33**, L743 (2000)
- 16 G.G. Paulus, F. Grasbon, H. Walther, P. Villorosi, M. Nisoli, S. Stagira, E. Priori, S. de Silvestri: *Nature* **414**, 182 (2001)
- 17 G. Paulus, F. Lindner, H. Walther, A. Baltuska, E. Goulielmakis, M. Lezius, F. Krausz: *Phys. Rev. Lett.* **91**, 253004 (2003)
- 18 F. Lindner, G.G. Paulus, H. Walter, A. Baltuska, E. Goulielmakis, M. Lezius, F. Krausz: *Ultrafast Opt.* **4**, 6 (2003)
- 19 G.G. Paulus, W. Nicklich, H. Xu, P. Lambropoulos, H. Walther: *Phys. Rev. Lett.* **72**, 2851 (1994)
- 20 S. Sartania, Z. Cheng, M. Lenzner, G. Tempea, C. Spielmann, F. Krausz, K. Ferencz: *Opt. Lett.* **22**, 1562 (1997)
- 21 M. Nisoli, S. de Silvestri, O. Svelto, R. Szípcos, K. Ferencz, C. Spielmann, S. Sartania, F. Krausz: *Opt. Lett.* **22**, 522 (1997)
- 22 V.S. Yakovlev, P. Dombi, G. Tempea, C. Lemell, J. Burgdörfer, T. Udem, A. Apolonski: *Appl. Phys. B: Lasers Opt.* **76**, 329 (2003)
- 23 C. Iaconis I. Walmsley: *J. Quant. Electron.* **35**, 501 (1999)
- 24 A. Apolonski, P. Dombi, G.G. Paulus, K. Torizuka, M. Kakehata, R. Holzwarth, T. Udem, C. Lemell, J. Burgdörfer, T.W. Hänsch, F. Krausz: *Phys. Rev. Lett.* **92**, 073902 (2004)
- 25 C.R. Gouy: *Acad. Sci. Paris* **110**, 1251 (1890)
- 26 A. Talebpour, C.Y. Chien, Y. Liang, S. Laroche, S.L. Chin: *J. Phys. B: At. Mol. Opt. Phys.* **30**, 1721 (1997)
- 27 G.P. Agrawal: *Nonlinear Fiber Optics* (Academic Press, San Diego 92101-4495, USA, 2nd ed. 1995)